

---

# Inferring community characteristics in labelled networks

---

**Anonymous Author(s)**

Affiliation  
Address  
email

## Abstract

1 Labelled networks form a very common and important class of data, naturally  
2 appearing in numerous applications in science and engineering. A typical inference  
3 goal is to determine how the vertex labels (called features) affect the network’s  
4 graph structure. A standard approach has been to partition the network into blocks  
5 grouped by distinct values of the feature of interest. A block-based random graph  
6 model – typically a variant of the stochastic block model (SBM) – is then used to  
7 test for evidence of asymmetric behaviour within these feature-based communities.  
8 Nevertheless, the resulting communities often do not produce a natural partition of  
9 the graph. In this work we introduce a new generative model, the feature-first block  
10 model (FFBM), which is more effective at describing vertex-labelled undirected  
11 graphs and also facilitates the use of richer queries on labelled networks. We  
12 develop a Bayesian framework for inference with this model, and we present a  
13 method to efficiently sample from the posterior distribution of the FFBM parame-  
14 ters. The FFBM’s structure is kept deliberately simple to retain easy interpretability  
15 of the parameter values. We apply the proposed methods to a variety of network  
16 data to extract the most important features along which the vertices are partitioned.  
17 The main advantages of the proposed approach are that the whole feature-space  
18 is used automatically, and features can be rank-ordered implicitly according to  
19 impact. Any features that do not significantly impact the high-level structure can  
20 be discarded to reduce the problem dimension. In cases where the vertex features  
21 available do not readily explain the community structure in the resulting network,  
22 the approach detects this and is protected against over-fitting. Results on several  
23 real-world datasets illustrate the performance of the proposed methods.

24 **1 Introduction**

25 A somewhat surprising property of many real-world networks is that they exhibit strong community  
26 structure; most nodes often belong to a densely connected cluster. There is high interest in recovering  
27 the latent communities from the observed graphs. The inferred communities can be exploited for  
28 compression algorithms [1] or used for link prediction in incomplete networks [4] to name a few  
29 applications.

30 We restrict our analysis to vertex-labelled networks. We shall refer to the vertex-labels as features. A  
31 common goal is to determine whether a given feature impacts graphical structure. To answer this  
32 from a Bayesian perspective we must use a random graph model; the standard is the stochastic block  
33 model (SBM) [8]. This is a latent variable model where each vertex belongs to a single block and the  
34 probability two nodes are connected depends only on the block memberships of each. There have

35 been many variants to this model – the most popular being the mixed-membership stochastic block  
 36 model (MMSBM) [2] and the overlapping stochastic block model (OSBM) [18]. Effectively, these  
 37 just extend the model to allow each vertex to belong to multiple blocks simultaneously. However,  
 38 a major drawback of these graphical models as applied to labelled networks is that they do not  
 39 automatically include vertex features in the random graph generation process. Approaches based on  
 40 graph neural networks [7] that utilise vertex features have been developed but these lack the easy  
 41 interpretability of the simpler models.

42 To analyse a labelled network using one of the simple SBM variants, a typical inference procedure  
 43 would be to partition the graph into blocks grouped by distinct values of the feature of interest. The  
 44 associated model can then be used to test for evidence of heterogeneous connectivity between the  
 45 feature-grouped blocks. Nevertheless, this approach is limited in that it can only consider one feature  
 46 at a time. This makes it difficult to rank order the features by magnitude of impact. Lastly, the  
 47 feature-grouped blocks are often an unnatural partition of the graph, leading to a poor model fit. We  
 48 would instead prefer to partition the graph into its most natural blocks and then find which of the  
 49 available features – if any – best predict the resulting partition.

50 With these desiderata in mind, we present a novel framework for modelling labelled networks, which  
 51 we call the feature-first block model (FFBM). This is an extension of the SBM to labelled networks.  
 52 We go on to present an efficient algorithm for sampling from the parameters of the feature-to-block  
 53 generator. We can interpret the sampled FFBM parameters to determine which features have the  
 54 largest impact on overall graphical structure.

## 55 2 Preliminaries

56 We first need a model for community-like structure in a network. For this we adopt the stochastic  
 57 block model (SBM) - widely used across academia. Each node in the graph belongs to a unique  
 58 community called a block. The probability that two nodes are connected depends only on the block  
 59 memberships of each. Specifically, we will use the microcanonical variant of the SBM, proposed by  
 60 Peixoto [13]. To allow for degree-variability between members of the same block, we must choose  
 61 the degree-corrected formulation (DC-SBM).

62 **Definition 2.1 (Microcanonical DC-SBM)** Let  $N \in \mathbb{Z}^+$  denote the number of vertices in an undi-  
 63 rected graph. The block memberships are encoded by a vector  $b \in [B]^N$ <sup>1</sup>, where  $B \in \mathbb{Z}^+$  is the  
 64 number of non-empty blocks. Let  $e \in (\mathbb{Z}_0^+)^{N \times N}$  be the matrix of edge counts between blocks.  $e_{rs}$  is  
 65 then the number of edges from block  $r$  onto block  $s$  – or twice that number if  $r = s$ . For undirected  
 66 graphs,  $e$  is symmetric. Let  $k \in (\mathbb{Z}_0^+)^N$  be a vector denoting the degree sequence of the graph.  $k_i$  is  
 67 then the degree of vertex  $i$ . The graph's adjacency matrix  $A \in \{0, 1\}^{N \times N}$  is generated as follows:

$$A \sim DC-SBM_{MC}(b, e, k) \quad (1)$$

68 Where edges are placed uniformly at random but respecting the constraints imposed by  $e$ ,  $b$  and  $k$  –  
 69 hence the microcanonical moniker. Specifically,  $A$  must satisfy the following:

$$e_{rs} = \sum_{i,j \in [N]} A_{ij} \mathbb{1}\{b_i = r\} \mathbb{1}\{b_j = s\} \quad \forall r, s \in [B] \quad \text{and} \quad k_i = \sum_{j \in [N]} A_{ij} \quad \forall i \in [N] \quad (2)$$

## 70 3 Feature-first block model

71 In this section we propose a novel generative model for labelled networks. We call this the feature-first  
 72 block model (FFBM) and outline its structure in 1 As before, we let  $N$  denote the number of nodes  
 73 and  $B$  the number of blocks in our graph. We define the vector  $x_i \in \mathcal{X}^D$  as the feature vector for the  
 74  $i$ 'th vertex.  $D$  is the number of features. For the datasets we analyse, we deal with binary feature

---

<sup>1</sup>We introduce the notation  $[K] := \{1, 2 \dots K\}$  to compactly define a set of  $K$  indices. Clearly,  $[K]$  is only defined for  $K \in \mathbb{Z}^+$ .

75 flags so  $\mathcal{X} = \{0, 1\}$ . The feature vectors  $\{x_i\}_{i=1}^N$  may be compactly subsumed into the feature matrix  
 76  $X \in \mathcal{X}^{N \times D}$ .

77 For the FFBM, we start with the feature matrix  $X$  and probabilistically generate a vector of block  
 78 memberships  $b \in [B]^N$ . The parameters of this step are encapsulated by  $\theta$ . Each feature vector  $x_i$  is  
 79 treated independently and used to generate the corresponding block membership  $b_i \in [B]$ . We choose  
 80 a single softmax layer to model  $p(b_i|x_i, \theta)$ . More complex models are possible but then deriving  
 81 meaning from the inferred parameter distributions is more difficult. Summarising, we write  $p(b|X, \theta)$   
 82 as follows:

$$p(b|X, \theta) = \prod_{i=1}^N p(b_i|x_i, \theta) = \prod_{i=1}^N \phi_{b_i}(x_i; \theta) = \prod_{i=1}^N \frac{\exp(w_{b_i}^T x_i)}{\sum_{k=1}^B \exp(w_k^T x_i)} \quad (3)$$

83 We deliberately exclude a bias term to ensure that the relationships we model are based on features  
 84 and not information about the size of each detected block; a more complete discussion on this topic  
 85 is given in A.5. The parameter vector  $\theta$  for this stage contains all the weight vectors  $\theta = \{w_k\}_{k=1}^B$ .  
 86 Each  $w_k$  has dimension  $D$ . We could instead write the parameters  $\theta$  as a  $B \times D$  matrix of weights  $W$ ;  
 87 this form has computational benefits as then  $z_i := Wx_i$ , which is the input to the softmax activation  
 88 function.

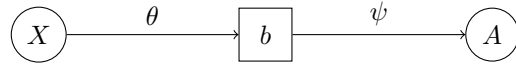


Figure 1: The feature-first block model (FFBM)

89 Once the block memberships  $b$  have been generated, we then draw the graph  $A$  from the microcanonical  
 90 DC-SBM (equation 4) with additional parameters encapsulated by  $\psi = \{\psi_e, \psi_k\}$ .

$$A \sim \text{DC-SBM}_{\text{MC}}(b, \psi_e, \psi_k) \quad (4)$$

### 91 3.1 Prior selection

92 Before performing any inference, we must specify priors on  $\theta$  and  $\psi$ . For  $\theta$  it seems sensible to  
 93 choose a Gaussian prior, with zero mean and variance matrix  $\sigma_\theta^2 I$  such that each element of  $\theta$  is  
 94 independent and distributed like  $\mathcal{N}(0, \sigma_\theta^2)$ . In vector form, the prior for  $\theta$  is therefore:

$$p(\theta) = \mathcal{N}(\theta; 0, \sigma_\theta^2 I) \quad (5)$$

95 In our model, the block memberships vector  $b$  is an intermediate latent variable and so we are not  
 96 free to choose a prior for it. Nevertheless, as far as inference on the right-hand-side of figure 1, we  
 97 regard  $p(b|X)$  as a pseudo-prior on  $b$ . We can show (appendix B.1) that our choice of prior for  $p(\theta)$   
 98 in equation 5 leads to a uniform  $p(b|X)$  in equation 6.

$$p(b|X) = \int p(b|X, \theta)p(\theta)d\theta = B^{-N} \quad (6)$$

99 This is an enormously important simplification as evaluating  $p(b|X)$  does not require an expensive  
 100 Monte-Carlo integration over the  $\theta$ -domain nor does it require the exact value of  $X$ . Peixoto  
 101 [13] proposes careful choices for the additional microcanonical SBM parameters  $\psi$  which we  
 102 adopt. Peixoto's idea is to write the joint prior on  $(b, e, k)$  as a product of conditionals  $p(b, e, k) =$   
 103  $p(b)p(e|b)p(k|e, b) = p(b)p(\psi|b)$ . For our purposes we must insert a conditioning on  $X$ , to form our  
 104 pseudo-prior for  $b$  and  $\psi$ , to give equation 7.

$$p(b, \psi|X) = p(b|X)p(\psi|b, X) = p(b|X)p(\psi|b) \quad (7)$$

105 Where we leverage the fact  $(\psi \perp\!\!\!\perp X)|b$ . We then borrow the priors proposed by Peixoto [13] for  
 106  $p(\psi|b)$  to complete our model. Please refer to appendix A.1 for the exact form of  $p(\psi|b)$ . All that  
 107 concerns the main argument is we have a computable form.

108 **4 Inference**

109 Now that we have defined the FFBM, we wish to leverage it to perform inference. Suppose we are  
110 presented with a vertex-labelled graph  $(A, X)$ ; the goal is to draw samples for  $\theta$  according to the  
111 posterior given the observed data:

$$\theta^{(t)} \sim p(\theta|A, X) \quad (8)$$

112 However, generating these samples is not easily done in practice. We therefore propose an iterative  
113 approach. We first draw samples  $b^{(t)}$  from the block membership posterior (equation 9) and then use  
114 each  $b^{(t)}$  to draw samples for  $\theta$  as in equation 10.

$$b^{(t)} \sim p(b|A, X) \quad (9)$$

$$\theta^{(t)} \sim p(\theta|X, b^{(t)}) \quad (10)$$

115 Both of these sampling steps can be implemented with a Markov Chain through the Metropolis-  
116 Hastings algorithm [5]. We just need to define a proposal distribution  $q(x, x')$  for proposing a move  
117  $x \rightarrow x'$  and be able to evaluate an un-normalised form of the target distribution, denoted  $\pi(\cdot)$ ,  
118 point-wise. The proposed move is then accepted with probability  $\alpha$  (equation 11) else it is rejected  
119 and we stay at  $x$ .

$$\alpha(x, x') = \min \left( \frac{\pi(x')q(x', x)}{\pi(x)q(x, x')}, 1 \right) \quad (11)$$

120 This accept-reject step ensures the resulting Markov Chain is in detailed balance with the target  
121 distribution  $\pi(\cdot)$ . What we propose in equations 9 and 10 is therefore implemented through a 2-level  
122 Markov chain. The resulting samples for  $\theta^{(t)}$  are unbiased in the sense that the expectation of their  
123 distribution is the posterior we are targeting:

$$\mathbb{E}_{b^{(t)}} \left[ p(\theta|X, b^{(t)}) \right] = \sum_{b \in [B]^N} p(\theta|X, b)p(b|A, X) = \sum_{b \in [B]^N} p(\theta, b|A, X) = p(\theta|A, X) \quad (12)$$

124 This is an example of a pseudo-marginal approach. Indeed, Andrieu and Roberts [3] show that the un-  
125 biased result in equation 12 is sufficient to prove that for large enough  $t$ ,  $\theta^{(t)} \sim \mathbb{E}_{b^{(t)}} [p(\theta|X, b^{(t)})] = p(\theta|A, X)$  which is exactly the distribution we are targeting (equation 8).

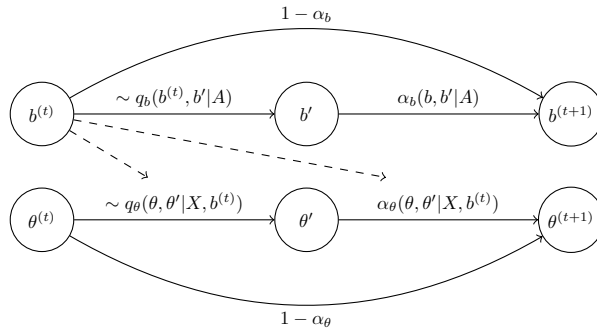


Figure 2: Sampling sequence

126  
127 The reason we split the Markov chain into two stages is because the summation over all latent states  
128  $b \in [B]^N$  required to directly compute the likelihood  $p(A|X, \theta) = \sum_{b \in [B]^N} p(A|b)P(b|X, \theta)$  is  
129 intractable –  $O(B^N)$ . Figure 2 shows an overview of the proposed method. We have introduced  
130 subscripts and conditionings to make explicit what variables each step utilises. We note the power of  
131 the simplification given by equation 6. As  $p(b|X)$  does not depend on the exact value of  $X$ , we do  
132 not need to know the value of  $X$  to perform the sampling on  $b$ . Conversely, for the  $\theta^{(t)}$  samples, we  
133 use only  $b^{(t)}$  but not  $A$  as  $(\theta \perp\!\!\!\perp A)|b$ .

134 **4.1 Sampling block memberships**

135 Peixoto [11] proposes a Monte Carlo method which we will base our approach on. It relies on writing  
 136 the posterior in the following form:

$$p(b|A, X) \propto p(A|b, X) \cdot p(b|X) = \pi_b(b) \quad (13)$$

137 Now  $\pi_b(\cdot)$  is the un-normalised density we wish to sample from for the  $b$ -chain. In other words, we  
 138 wish to construct a Markov chain that has  $\pi_b(\cdot)$  as its invariant distribution. We can break  $\pi_b$  down as  
 139 follows:

$$\pi_b(b) = p(b|X) \sum_{\psi} p(A, \psi|b, X) = p(b|X)p(A, \psi^*|b, X) = p(A|b, \psi^*) \cdot p(\psi^*|b) \cdot p(b|X) \quad (14)$$

140 Since we are using the microcanonical SBM formulation, there is only one value of  $\psi$  that is  
 141 compatible with the given  $(A, b)$  pair (given in equation 2). We denote this value  $\psi^* = \{\psi_k^*, \psi_e^*\}$ .  
 142 Therefore, the summation over all  $\psi$  reduces to just the single  $\psi^*$  term; this is the power of the  
 143 microcanonical formulation. We also define the microcanonical entropy of the configuration as.

$$S(b) = -\log \pi_b(b) = -\left( \log p(A|b, \psi^*) + \log p(\psi^*, b|X) \right) \quad (15)$$

144 This entropy can equally be thought of as the description length of the graph. The exact form of  
 145 the proposal  $q_b$  is explored thoroughly by Peixoto [11] and not repeated here. There is a widely  
 146 used library for Python made available under LGPL called `graph-tool` [12], which implements this  
 147 algorithm. The only modification we make is in the block membership prior  $p(b)$  which we replace  
 148 with  $p(b|X) = B^{-N}$ , which cancels out in the MH accept-reject step as it is independent of  $b$ .

149 **4.2 Sampling feature-to-block generator parameters**

150 The invariant distribution we wish to target for the  $\theta$  samples is the posterior of  $\theta$  given the values of  
 151 the pair  $(X, b)$ . We write this as follows:

$$\pi_\theta(\theta) \propto p(\theta|X, b) \propto p(b|X, \theta)p(\theta) \propto \pi_\theta(\theta) \propto \exp(-U(\theta)) \quad (16)$$

152 Where we have introduced  $U(\theta)$  equal to the negative log posterior. We define  $y_{ij} := \mathbb{1}\{b_i = j\}$  and  
 153  $a_{ij} := \phi_j(x_i; \theta)$ . Discarding constant terms, we can write  $U(\theta)$  as in equation 17 (refer to appendix  
 154 B.2 for the derivation).

$$U(\theta) = \left( \sum_{i=1}^N \sum_{j=1}^B y_{ij} \log \frac{1}{a_{ij}} \right) + \frac{1}{2\sigma_\theta^2} \|\theta\|^2 = N \cdot \mathcal{L}(\theta) + \frac{1}{2\sigma_\theta^2} \|\theta\|^2 \quad (17)$$

155  $U(\theta)$  in equation 17 appears a typical objective function for neural network training. The first term  
 156 is introduced by the likelihood. We collect it into  $N \cdot \mathcal{L}(\theta)$ , which is the cross-entropy between the  
 157 graph-predicted and feature-predicted block memberships summed over all vertices. The second  
 158 term of equation 17 – introduced by the prior – brings a form of regularisation, guarding against  
 159 over-fitting. Different to traditional applications, our goal is not to find the minimiser of  $U(\theta)$  but to  
 160 draw samples from the posterior  $\pi_\theta(\cdot) \propto \exp(-U(\cdot))$ . We can use  $\nabla U$  as a useful heuristic to bias  
 161 our proposal towards regions of higher target density. We therefore adopt the Metropolis-adjusted  
 162 Langevin algorithm (MALA) – first proposed by Roberts and Tweedie [15]. Given the current sample  
 163  $\theta$ , we generate a new sample  $\theta'$  according to equation 18.

$$\theta' = \theta - h \nabla U(\theta) + \sqrt{2h} \cdot \xi \quad (18)$$

$$\therefore q_\theta(\theta, \theta') = \mathcal{N}(\theta'; \theta - h \nabla U(\theta), 2hI) \quad (19)$$

164 Where  $\xi \sim \mathcal{N}(0, I)$  and  $h$  is a step-size parameter – which may vary with the sample index (appendix  
 165 A.2 explores this more fully). Without the injected noise term, MALA is equivalent to gradient  
 166 descent. We require the noise term  $\xi$  to fully explore the parameter space. We can write the proposal  
 167 distribution  $q_\theta$  as in equation 19. The term  $\nabla U$  has an easy to compute analytic form (derived in  
 168 Appendix B.3). By noting that  $\theta = \{w_k\}_{k=1}^B$ , we write the derivative with respect to each  $w_k$  as:

$$\frac{\partial U}{\partial w_k} = - \left( \sum_{i=1}^N \left\{ \tilde{x}_i (y_{ik} - a_{ik}) \right\} - \frac{w_k}{\sigma_\theta^2} \right) \quad (20)$$

169 After a proposed move is generated, in typical Metropolis-Hastings fashion we accept the move with  
 170 probability  $\alpha_\theta$ , as in equation 11.

171 **4.3 Sampling sequence**

172 Up to this point, each  $\theta^{(t)}$  update uses its corresponding  $b^{(t)}$  sample. This means that the evaluation  
 173 of  $U(\theta)$  and  $\nabla U(\theta)$  has high variance. This may lead to longer burn-in for the resulting Markov  
 174 chain. The only link between  $b^{(t)}$  and  $\theta^{(t)}$  is in the evaluation of  $U(\theta)$  and  $\nabla U(\theta)$  which depends  
 175 only on the matrix  $y^{(t)}$  with entries  $y_{ij}^{(t)} := \mathbb{1}\{b_i^{(t)} = j\}$ . We would rather deal with the expectation  
 176 of each  $y_{ij}^{(t)}$ :

$$\mathbb{E} [y_{ij}^{(t)}] = \mathbb{E}_{b^{(t)}} [\mathbb{1}(b_i^{(t)} = j)] = p(b_i = j | A, X) \quad (21)$$

177 We can obtain an unbiased estimate for this quantity using the set of  $b$ -samples. However, as with  
 178 all MCMC methods, we must only use samples after burn-in and thinning have been applied. We  
 179 introduce  $\mathcal{T}_b$  to denote the retained set of indices for the  $b$ -samples and  $\mathcal{T}_\theta$  similarly for the  $\theta$ -chain.  
 180 An in-depth discussion of how these sets are chosen is given in appendix A.3. The unbiased estimate  
 181 for  $y_{ij}^{(t)}$  using the restricted sample set  $\mathcal{T}_b$  is denoted  $\hat{y}_{ij}$  and has form:

$$\hat{y}_{ij} := \frac{1}{|\mathcal{T}_b|} \sum_{t \in \mathcal{T}_b} y_{ij}^{(t)} = \frac{1}{|\mathcal{T}_b|} \sum_{t \in \mathcal{T}_b} \mathbb{1}\{b_i^{(t)} = j\} \quad (22)$$

182 We choose to feed each  $\theta^{(t)}$  update step the same matrix  $\hat{y}$  for all  $t$  rather than the corresponding  $y^{(t)}$ .  
 183 This means we no longer need to run the  $b$  and  $\theta$  Markov chains concurrently. Instead, we run the  
 184  $b$ -chain to completion and use it to generate  $\hat{y}$ . This affords us the flexibility to vary the lengths of the  
 185  $b$  and  $\theta$ -chains. Furthermore, the changeover from  $y^{(t)}$  to  $\hat{y}$  reduces the burn-in time for the  $\theta$ -chain  
 186 by reducing the variance in our evaluation of  $U$  and  $\nabla U$ . A description of the overall algorithms is  
 187 given in appendix C.1.

188 **4.4 Dimensionality reduction**

189 Once we have the samples  $\{\theta^{(t)}\} \sim p(\theta | A, X)$ , we can compute the empirical mean and standard  
 190 deviation of each component of  $\theta$ . Switching back to matrix notation we define  $\theta = W$ , such that  
 191  $W_{ij}$  is the weight component for block  $i$  and feature  $j$ , we can define:

$$\hat{\mu}_{ij} := \frac{1}{|\mathcal{T}_\theta|} \sum_{t \in \mathcal{T}_\theta} W_{ij}^{(t)} \quad \text{and} \quad \hat{\sigma}_{ij}^2 := \frac{1}{|\mathcal{T}_\theta|} \sum_{t \in \mathcal{T}_\theta} \left( W_{ij}^{(t)} - \hat{\mu}_{ij} \right)^2 \quad (23)$$

192 A simple heuristic to discard the least important features requires specifying a cutoff  $c > 0$  and a  
 193 multiplier  $k > 0$ . We define the function  $\mathcal{F}_i(j)$  as in 24 then only keep features with indices  $d \in \mathcal{D}'$ ,  
 194 where  $\mathcal{D}'$  is constructed as in equation 25.

$$\mathcal{F}_i(j) := (\hat{\mu}_{ij} - k\hat{\sigma}_{ij}, \hat{\mu}_{ij} + k\hat{\sigma}_{ij}) \cap (-c, +c) \quad (24)$$

$$\mathcal{D}' := \{j \in [D] : \exists i \in [B] \text{ s.t. } \mathcal{F}_i(j) \neq \emptyset\} \quad (25)$$

195 Intuitively, this means discarding any feature for which  $\hat{\mu}_{ij} \pm k\hat{\sigma}_{ij}$  lies within or spans the null  
 196 region  $(-c, c)$  for all block indices. If we were to use the Laplace approximation for the posterior  
 197  $p(W_{ij} | A, X) \approx \mathcal{N}(W_{ij}; \mu_{ij}, \sigma_{ij}^2)$ , then this is effectively a hypothesis test on the value of  $W_{ij}$   
 198 (equation 26).  $\mathcal{D}'$  then comprises all features  $i$  for which  $H_1$  is accepted at least once for some  
 199  $j \in [B]$ .

$$H_0 : |W_{ij}| \leq c \quad H_1 : |W_{ij}| > c \quad (26)$$

200 The multiplier  $k$  determines the degree of significance of the result. However, as the Laplace  
 201 approximation is not exact we will only treat this dimensionality reduction method as a useful  
 202 heuristic and not an exact method. Conversely, we could fix  $k = k_0$  and the dimension of our reduced  
 203 feature set  $|\mathcal{D}'| = D'$ . We would then like to find the largest value of  $c$  such that  $|\mathcal{D}'| = D'$  given  
 204  $k = k_0$ . This is summarised in equation 27. This approach is often preferred as it fixes the number of  
 205 reduced dimensions.

$$c^* = \arg \max_{c>0} (c : |\mathcal{D}'| = D', k = k_0) \quad (27)$$

206 For an algorithmic implementation of this method refer to appendix C.1.

207 **5 Experiments**

208 We apply the developed methods to a variety of datasets. These are chosen to span a range of node  
 209 counts  $N$ , edge counts  $E$  and feature space dimension  $D$ . We consider the following:

- 210 • **Political books** [9] ( $N = 105, E = 441, D = 3$ ) – network of Amazon book sales about U.S.  
 211 politics, published close to the presidential election in 2004. Two books are connected if they were  
 212 frequently co-purchased by customers. Vertex features encode the political affiliation of the author  
 213 (liberal, conservative or neutral).
- 214 • **Primary school dynamic contacts** [16] ( $N = 238, E = 5539, D = 13$ ) – network of face-to-face  
 215 contacts amongst students and teachers at a primary school in Lyon, France. Two nodes are  
 216 connected if the two parties shared a face-to-face interaction over the school-day. Vertex features  
 217 include class membership (one of 10 values: 1A-5B), gender (male, female) and teacher status  
 218 encoded as an 11th school-class. No further identifiable information is retained. We choose to  
 219 analyse just the second day of results.
- 220 • **Facebook egonet** [6] ( $N = 747, E = 30025, D = 480$ ) – an assortment of Facebook users'  
 221 friends lists. Vertex features are extracted from each user's profile and are fully anonymised. They  
 222 include information about education history, languages spoken, gender, home-town, birthday etc.  
 223 We focus on the egonet with id 1912.

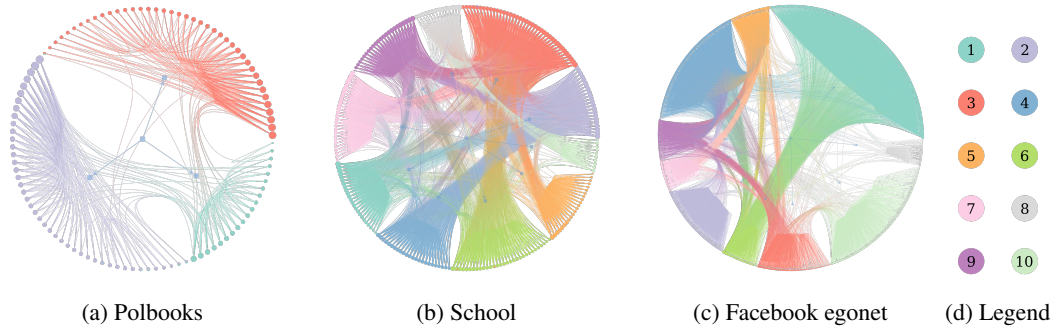


Figure 3: Networks laid out and coloured according by inferred block memberships  $\hat{y}$  for a given experiment iteration. Visualisation performed using *graph-tool* [12]

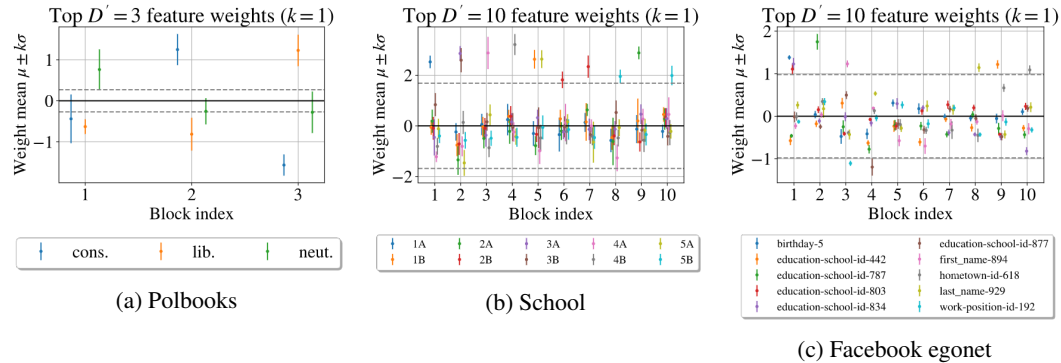


Figure 4: Reduced dimension feature-to-block generator weight samples

224 We require metrics to assess performance. This can be split into two separate components: the  
 225 microcanonical SBM fit (concerned with the  $b$ -samples) and the fit of the feature-to-block generator  
 226 (concerned with the  $\theta$ -samples). Starting with the SBM,  $S(b)$  (equation 15) can be interpreted as  
 227 the description length of the partition imposed by  $b$ . It is only natural to divide this quantity by the  
 228 number of entities (nodes and edges) in our graph  $N + E$  to allow for rough comparison between

Table 1: Experimental results averaged over  $n = 10$  iterations (mean  $\pm$  standard deviation)

| Dataset   | $B$ | $D$ | $D'$ | $\bar{S}_e$       | $\bar{\mathcal{L}}_0$ | $\bar{\mathcal{L}}_1$ | $c^*$             | $\bar{\mathcal{L}}'_0$ | $\bar{\mathcal{L}}'_1$ |
|-----------|-----|-----|------|-------------------|-----------------------|-----------------------|-------------------|------------------------|------------------------|
| Polbooks  | 3   | 3   | —    | $2.250 \pm 0.000$ | $0.563 \pm 0.042$     | $0.595 \pm 0.089$     | —                 | —                      | —                      |
| School    | 10  | 13  | 10   | $1.894 \pm 0.004$ | $0.787 \pm 0.127$     | $0.885 \pm 0.129$     | $1.198 \pm 0.249$ | $0.793 \pm 0.132$      | $0.853 \pm 0.132$      |
| FB egonet | 10  | 480 | 10   | $1.626 \pm 0.003$ | $1.326 \pm 0.043$     | $1.538 \pm 0.069$     | $0.94 \pm 0.019$  | $1.580 \pm 0.150$      | $1.605 \pm 0.106$      |

graphs. This defines a simple metric to gauge the fit of the SBM: the description length per entity averaged over the  $b$ -samples (equation 28):

$$\bar{S}_e := \frac{1}{(N+E)|\mathcal{T}_b|} \sum_{t \in \mathcal{T}_b} S(b^{(t)}) \quad (28)$$

However, to assess the performance of the feature-to-block predictor, we must partition the vertex set  $[N]$  into training and test sets. We choose to randomly partition the vertices on each experiment run such that a constant fraction  $f$  of the available vertices go to form our training set  $\mathcal{G}_0$  and the remainder are held out to form our test set  $\mathcal{G}_1$ . The  $b$ -chain is run using the whole network but we only use vertices  $v \in \mathcal{G}_0$  to train the  $\theta$ -chain. As  $|\mathcal{G}_0| \neq |\mathcal{G}_1|$  in general, we cannot use the un-normalised log target  $U$  (equation 17) for comparison as the total cross-entropy loss is scaled by the size of each set but the prior term stays constant. We therefore must use the average cross-entropy loss over each set (equation 29):

$$\bar{\mathcal{L}}_\star := \frac{1}{|\mathcal{T}_\theta|} \sum_{t \in \mathcal{T}_\theta} \mathcal{L}_\star(\theta^{(t)}) \quad \text{where} \quad \mathcal{L}_\star(\theta^{(t)}) := \frac{1}{|\mathcal{G}_\star|} \sum_{i \in \mathcal{G}_\star} \sum_{j \in [B]} \hat{y}_{ij} \log \frac{1}{\phi_j(x_i; \theta^{(t)})} \quad (29)$$

Where  $\star \in \{0, 1\}$  has been introduced to toggle between training and test sets. Table 1 summarises the results for each experiment.<sup>2</sup> We also apply the dimensionality reduction method on the two higher dimensional datasets (the school and FB egonet). For this we leverage equation 27, to reduce the dimension from  $D$  to  $D'$  with  $k = 1$  to yield the maximal cutoff  $c^*$ . We then retrain the feature-block predictor using just the retained feature set  $D'$  and report the loss over the training and test sets for the reduced classifier – denoted  $\bar{\mathcal{L}}'_0$  and  $\bar{\mathcal{L}}'_1$  respectively. These values are also included in table 1.

Table 1 already highlights some general trends in the results. Firstly, the variance of the test loss  $\bar{\mathcal{L}}_1$  tends to be higher than the training loss  $\bar{\mathcal{L}}_0$ . This is expected as our test set is smaller than the training set and so more susceptible to variability in its construction. Indeed, most of the variance in the evaluation of  $\bar{\mathcal{L}}_0$  and  $\bar{\mathcal{L}}_1$  comes from the random partitioning of the graph into training and test sets. Secondly, it can be seen that the dimensionality reduction procedure brings the training and test losses closer together. This implies that the features we keep are indeed correlated with the underlying graphical partition and that the approach generalises correctly.

The average description length per entity of the graph  $\bar{S}_e$  has very low variance implying the detected communities can be found reliably (to within an arbitrary relabelling of blocks). For reference we plot an inferred partition for each of the graphs on figure 3. The polbooks graph yields the cleanest separation between blocks but nonetheless the inferred partitions for the other datasets do succeed at partitioning the graph into densely connected clusters.

## 5.1 Political books

We wish to determine whether the author’s political affiliation is a good predictor of the overall network structure. We choose to partition the network into  $B = 3$  communities as we only have this many distinct values for political affiliation (conservative, liberal or neutral). From, figure 4a, we see that all 3 blocks have a distinct political affiliation as their largest positive component. This is strong evidence that political affiliation is indeed the axis which best predicts the 3-way natural partition of the graph into blocks. Furthermore, from table 1 we see that the training and test losses are very similar and both are low in magnitude. This provides further evidence to the claim that political affiliation is the best explanatory variable for the overall network structure.

<sup>2</sup>For a comprehensive list of the hyper-parameters used for each experiment please see appendix C.2

266 **5.2 Primary school dynamic contacts**

267 We choose  $B = 10$  in line with the total number of school-classes. As before, we sample the  
268 block-generator parameters  $\theta$  and employ the dimensionality reduction technique with standard  
269 deviation multiplier  $k = 1$  to pick out the top  $D' = 10$  features. We then plot the weights for the  
270 surviving features  $d \in D'$  on figure 4b. Immediately, we see that only the pupils' class memberships  
271 have survived (1A-5B); gender and teacher/student status have been discarded meaning that these are  
272 not good predictors of overall macro-structure.

273 The vast majority of blocks are composed of a single class. However, some blocks have 2 comparably  
274 good classes as their predictor. For example, block 2 contains classes 3A and 3B as its 2 best  
275 predictors. This suggests that the social divide between classes is less pronounced for pupils in year  
276 3. Conversely, some classes are found to extend over two detected blocks (class 2B spans blocks 6  
277 and 7) but we nonetheless do not have a feature which explains the division. The most surprising  
278 block is number 5 - which has comparable weightings for classes 5A and 1B. Perhaps there was a  
279 joint event between those two classes on the day the data were collected.

280 **5.3 Facebook egonet**

281 We choose  $B = 10$  and  $D' = 10$  for this experiment. The remaining features (figure 4c) are those  
282 that best explain the high-level community structure. The majority of the surviving features are  
283 education related. Nevertheless, for  $D' = 10$  we only have good explanations for the makeup of  
284 some of the detected blocks; several blocks in figure 4c do not have high-magnitude components for  
285  $D' = 10$ .

286 When the feature dimension is very large, it becomes increasingly likely that a particular feature may  
287 uniquely identify a small set of nodes. If these nodes are all part of the same community then the  
288 classifier will overfit for that particular parameter. The regularisation term imposed by the prior goes  
289 some way to alleviating this problem. Nevertheless, we see in figure 4c that the feature `birthday-5`  
290 has a very high weight as it relates to block 1 – but it would be preposterous to conclude that birthdays  
291 determine graphical structure. The analyst must remain vigilant of such problems.

292 **6 Conclusion**

293 The FFBM was developed to address the shortcomings of other graphical models when testing how  
294 vertex features affect community structure. The idea is to divide the graph into its most natural  
295 partition and test whether the vertex features can accurately explain this partition. It is very easy to  
296 find vertex features that are in some way correlated with the graphical structure. Nonetheless, only  
297 when we find the feature that best describes the most pronounced partition do we have a stronger  
298 case for causation.

299 With the newly-defined FFBM, we go on to present an efficient inference algorithm to sample the  
300 parameters  $\theta$  of the feature-to-block generator. This is introduced as two concurrent Markov chains  
301 to sample the block memberships  $b$  and block generator parameters  $\theta$ . Nevertheless, we can serialise  
302 the chains and use the empirical mean of the  $b$ -samples as the input to our  $\theta$ -chain. This reduces the  
303 variance in our evaluation of the target distribution and thus shortens burn-in.

304 The overall method is shown to be effective at extracting and describing the most natural communities  
305 in a labelled network. Nevertheless, the approach can only currently explain the structure at the  
306 macro-scale. We cannot explain structure within each block. Future work will benefit from extending  
307 the FFBM to be hierarchical in nature. That way, the structure of the network can be explained at all  
308 length-scales of interest. So long as data collection techniques remain ethical and care is taken to  
309 respect personal privacy, such empowered decision-making can only help humankind.

310 **References**

- 311 [1] Emmanuel Abbe. Graph compression: The effect of clusters. In *2016 54th Annual Allerton  
312 Conference on Communication, Control, and Computing (Allerton)*, pages 1–8, 2016. doi:  
313 10.1109/ALLERTON.2016.7852203.
- 314 [2] Edo M Airoldi, David Blei, Stephen Fienberg, and Eric Xing. Mixed membership  
315 stochastic blockmodels. In D. Koller, D. Schuurmans, Y. Bengio, and L. Bottou,  
316 editors, *Advances in Neural Information Processing Systems*, volume 21. Curran As-  
317 sociates, Inc., 2009. URL <https://proceedings.neurips.cc/paper/2008/file/8613985ec49eb8f757ae6439e879bb2a-Paper.pdf>.
- 319 [3] Christophe Andrieu and Gareth O. Roberts. The pseudo-marginal approach for efficient Monte  
320 Carlo computations. *The Annals of Statistics*, 37(2):697 – 725, 2009. doi: 10.1214/07-AOS574.  
321 URL <https://doi.org/10.1214/07-AOS574>.
- 322 [4] Solenne Gaucher, Olga Klopp, and Geneviève Robin. Outliers detection in networks with  
323 missing links, 2020.
- 324 [5] W. K. Hastings. Monte carlo sampling methods using markov chains and their applications.  
325 *Biometrika*, 57(1):97–109, 1970. ISSN 00063444. URL <http://www.jstor.org/stable/2334940>.
- 327 [6] Jure Leskovec and Julian Mcauley. Learning to discover social circles in ego net-  
328 works. In F. Pereira, C. J. C. Burges, L. Bottou, and K. Q. Weinberger, ed-  
329 itors, *Advances in Neural Information Processing Systems*, volume 25. Curran As-  
330 sociates, Inc., 2012. URL <https://proceedings.neurips.cc/paper/2012/file/7a614fd06c325499f1680b9896beedeb-Paper.pdf>.
- 332 [7] Nikhil Mehta, Lawrence Carin Duke, and Piyush Rai. Stochastic blockmodels meet graph  
333 neural networks. In Kamalika Chaudhuri and Ruslan Salakhutdinov, editors, *Proceedings of the  
334 36th International Conference on Machine Learning*, volume 97 of *Proceedings of Machine  
335 Learning Research*, pages 4466–4474. PMLR, 09–15 Jun 2019. URL <http://proceedings.mlr.press/v97/mehta19a.html>.
- 337 [8] Krzysztof Nowicki and Tom A. B Snijders. Estimation and prediction for stochastic block-  
338 structures. *Journal of the American Statistical Association*, 96(455):1077–1087, 2001. doi:  
339 10.1198/016214501753208735. URL <https://doi.org/10.1198/016214501753208735>.
- 340 [9] Boris Pasternak and Ivor Ivask. Four unpublished letters. *Books Abroad*, 44(2):196–200, 1970.  
341 ISSN 00067431. URL <http://www.jstor.org/stable/40124305>.
- 342 [10] Tiago P. Peixoto. Parsimonious module inference in large networks. *Physical Review Letters*,  
343 110(14), Apr 2013. ISSN 1079-7114. doi: 10.1103/physrevlett.110.148701. URL <http://dx.doi.org/10.1103/PhysRevLett.110.148701>.
- 345 [11] Tiago P. Peixoto. Efficient monte carlo and greedy heuristic for the inference of stochastic  
346 block models. *Physical Review E*, 89(1), Jan 2014. ISSN 1550-2376. doi: 10.1103/physreve.89.  
347 012804. URL <http://dx.doi.org/10.1103/PhysRevE.89.012804>.
- 348 [12] Tiago P. Peixoto. The graph-tool python library. *figshare*, 2014. doi: 10.6084/m9.figshare.  
349 1164194. URL [http://figshare.com/articles/graph\\_tool/1164194](http://figshare.com/articles/graph_tool/1164194).
- 350 [13] Tiago P. Peixoto. Nonparametric bayesian inference of the microcanonical stochastic block  
351 model. *Physical Review E*, 95(1), Jan 2017. ISSN 2470-0053. doi: 10.1103/physreve.95.012317.  
352 URL <http://dx.doi.org/10.1103/PhysRevE.95.012317>.
- 353 [14] Jaakko Riihimäki and Aki Vehtari. Laplace approximation for logistic gaussian process density  
354 estimation and regression, 2013.

- 355 [15] Gareth O. Roberts and Richard L. Tweedie. Exponential convergence of Langevin distributions  
356 and their discrete approximations. *Bernoulli*, 2(4):341 – 363, 1996. doi: [bj/1178291835](https://doi.org/10.1177/092620059600200402). URL  
357 [https://doi.org/](https://doi.org/10.1177/092620059600200402).
- 358 [16] Juliette Stehlé, Nicolas Voirin, Alain Barrat, Ciro Cattuto, Lorenzo Isella, Jean-François Pinton,  
359 Marco Quaggiotto, Wouter Van den Broeck, Corinne Régis, Bruno Lina, and Philippe Vanhems.  
360 High-resolution measurements of face-to-face contact patterns in a primary school. *PLoS ONE*,  
361 6(8):1–13, 08 2011. doi: [10.1371/journal.pone.0023176](https://doi.org/10.1371/journal.pone.0023176). URL <https://doi.org/10.1371/journal.pone.0023176>.
- 363 [17] Max Welling and Yee Whye Teh. Bayesian learning via stochastic gradient langevin dynam-  
364 ics. In *Proceedings of the 28th International Conference on International Conference on*  
365 *Machine Learning*, ICML’11, page 681–688, Madison, WI, USA, 2011. Omnipress. ISBN  
366 9781450306195.
- 367 [18] Jun Zhu, Jiaming Song, and Bei Chen. Max-margin nonparametric latent feature models for  
368 link prediction, 2016.

369    **Checklist**

- 370    1. For all authors...
- 371        (a) Do the main claims made in the abstract and introduction accurately reflect the paper's  
372              contributions and scope? [Yes] See experiments section 5
- 373        (b) Did you describe the limitations of your work? [Yes] See conclusion 6 and experiments  
374              5 sections
- 375        (c) Did you discuss any potential negative societal impacts of your work? [Yes] See  
376              conclusion 6
- 377        (d) Have you read the ethics review guidelines and ensured that your paper conforms to  
378              them? [Yes]
- 379    2. If you are including theoretical results...
- 380        (a) Did you state the full set of assumptions of all theoretical results? [Yes] See inference  
381              section 4
- 382        (b) Did you include complete proofs of all theoretical results? [Yes] See inference section  
383              4
- 384    3. If you ran experiments...
- 385        (a) Did you include the code, data, and instructions needed to reproduce the main experi-  
386              mental results (either in the supplemental material or as a URL)? [Yes] See supplemen-  
387              tary code
- 388        (b) Did you specify all the training details (e.g., data splits, hyperparameters, how they  
389              were chosen)? [Yes] See appendix C.2
- 390        (c) Did you report error bars (e.g., with respect to the random seed after running experi-  
391              ments multiple times)? [Yes] See table 1
- 392        (d) Did you include the total amount of compute and the type of resources used (e.g., type  
393              of GPUs, internal cluster, or cloud provider)? [Yes] See appendix C.3
- 394    4. If you are using existing assets (e.g., code, data, models) or curating/releasing new assets...
- 395        (a) If your work uses existing assets, did you cite the creators? [Yes] See section experi-  
396              ments 5
- 397        (b) Did you mention the license of the assets? [Yes] See section inference 4
- 398        (c) Did you include any new assets either in the supplemental material or as a URL? [Yes]  
399              Supplementary material
- 400        (d) Did you discuss whether and how consent was obtained from people whose data you're  
401              using/curating? [Yes] Referred to original papers
- 402        (e) Did you discuss whether the data you are using/curating contains personally identifiable  
403              information or offensive content? [Yes] Referred to original papers
- 404    5. If you used crowdsourcing or conducted research with human subjects...
- 405        (a) Did you include the full text of instructions given to participants and screenshots, if  
406              applicable? [N/A]
- 407        (b) Did you describe any potential participant risks, with links to Institutional Review  
408              Board (IRB) approvals, if applicable? [N/A]
- 409        (c) Did you include the estimated hourly wage paid to participants and the total amount  
410              spent on participant compensation? [N/A]

411 **A Appendix: Additional material**

412 **A.1 SBM likelihood and prior**

413 For reference, we provide the likelihoods and priors for the mircocanonical SBM proposed by Peixoto  
414 [13]. We have that the graph  $A$  is drawn from the SBM:

$$A \sim \text{DC-SBM}_{\text{MC}}(b, e, k) \quad (30)$$

415 With edges placed uniformly at random but respecting the constraints imposed by  $b, e$  and  $k$ . The  
416 likelihood calculation for  $p(A|k, e, b)$  then reduces to a case of counting configurations that yield  
417 the same adjacency matrix,  $\Xi(A)$ , and dividing by the total number of configurations possible,  $\Xi(e)$ .  
418 This is why this formulation is given the microcanonical moniker. If we consider the half-edges to be  
419 distinguishable for a moment, the total number of configurations that satisfy the  $e$  constraint is:

$$\Omega(e) = \frac{\prod_r e_r!}{\prod_{r,s:r < s} e_{rs}! \cdot \prod_r e_{rr}!!} \quad (31)$$

420 Where  $e_r := \sum_s e_{rs}$  and  $(2m)!! := 2^m m!$ . Nevertheless, a great number of these configurations  
421 yield the same graph  $A$ . We denote the number of configurations that yield the adjacency matrix  $A$   
422 with  $\Xi(A)$ , which can be computed as:

$$\Xi(A) := \frac{\prod_i k_i!}{\prod_{i,j : i < j} A_{ij}! \prod_i A_{ii}!!} \quad (32)$$

423 Note the similarity between the forms of  $\Omega(e)$  and  $\Xi(A)$  as  $e$  is effectively the adjacency matrix of  
424 the block-graph. With these defined we can write the overall likelihood:

$$p(A|k, e, b) = \frac{\Xi(A)}{\Omega(e)} \quad (33)$$

425 Obviously, this form is only defined if  $A$  respects the constraints imposed by  $(k, e, b)$  else the  
426 likelihood is 0. With the likelihood defined, we move on to the prior. As discussed in the main text,  
427 for the FFBM  $b$  is an intermediate variable and not a parameter so we are not free to choose a prior  
428 for it. Nevertheless, we can borrow the conditional prior proposed by Peixoto [13] for  $p(e, k|b)$ :

$$p(e, k|b) = p(e|b)p(k|e, b) = \left[ \begin{Bmatrix} \{ \frac{B}{2} \} \\ E \end{Bmatrix} \right]^{-1} \cdot \left[ \prod_r \frac{\prod_j \eta_j^r!}{n_r! q(e_r, n_r)} \right] \quad (34)$$

429 Where  $\{ \frac{n}{m} \}$  is shorthand for  $\binom{n+m-1}{m} = \frac{(n+m-1)!}{(n-1)!(m)!}$  which can be thought of as the total number  
430 of distinct histograms with  $n$  bins under the constraint they sum to  $m$ .  $E = \frac{1}{2} \sum_{r,s} e_{rs}$  is the total  
431 number of edges in the graph. Importantly,  $E$  is not allowed to vary and so  $p(e|b)$  is uniform with  
432 respect to  $e$ . The variable  $\eta_j^r$  is introduced to denote the number of vertices in block  $r$  that have degree  
433  $j$ . Formally,  $\eta_j^r := \sum_i \mathbb{1}\{b_i = r\} \mathbb{1}\{k_i = j\}$ . Furthermore,  $q(m, n)$  is the number of different  
434 histograms with at most  $n$  non-zero bins that sum to  $m$ .  $q(m, n)$  is related to but different from  $\{ \frac{n}{m} \}$ .  
435 Recall that  $e_r := \sum_s e_{rs}$  is the total number of half edges in block  $r$  and  $n_r := \sum_i \mathbb{1}\{b_i = r\}$  is the  
436 number of vertices assigned to block  $r$ .

437 The form of these priors were chosen carefully by Peixoto [13] to more closely match the structure of  
438 empirical networks than simple uniform priors. We do not repeat his arguments here.

439 **A.2 Choosing the MALA step-size**

440 For sampling from the  $\theta$ -chain of the block membership generator parameters, we employed the  
441 Metropolis Adjusted Langevin Algorithm (MALA). At iteration  $t$ , the proposed sample is generated  
442 by:

$$\theta' = \theta^{(t)} - h_t \nabla U(\theta^{(t)}) + \sqrt{2h_t} \cdot \xi \quad (35)$$

443 There are two competing objectives when choosing the step-size  $h_t$ . On the one hand, we want the  
444 step-size to be large so that we arrive at a high density region quickly. However, too large a step-size

445 will lead to a lower acceptance ratio and thus inefficient sampling. A solution to this problem would  
446 be to slowly decrease the step-size with  $t$  - often called simulated annealing. Therefore, we still have  
447 a short burn-in time but will not bounce around the mode for large  $t$ . As well as the trivial constraint  
448 for  $h_t$  to be strictly positive, we introduce two further constraints as outlined by Welling and Teh  
449 [17]:

$$\sum_{t=1}^{\infty} h_t = \infty \quad \text{and} \quad \sum_{t=1}^{\infty} h_t^2 < \infty \quad (36)$$

450 The first constraint ensures that we have cover sufficient distance to arrive at any arbitrary point in  
451 our domain, no matter the starting point. The second constraint ensures that once we converge to the  
452 mode rather than simply bouncing around it. Welling and Teh [17] propose the following form for a  
453 polynomially decaying step-size which we adopt:

$$h_t = \alpha(\beta + t)^{-\gamma} \quad (37)$$

454 Where  $\alpha, \beta, \gamma$  are hyper-parameters to be chosen. We require  $\alpha, \beta > 0$  and  $\gamma \in (0.5, 1]$  to satisfy  
455 equation 36. To reduce the number of hyperparameters we set these to have values given by the  
456 equations 38.

$$\alpha = \frac{250 \cdot s}{N} \quad \beta = 1000 \quad \gamma = 0.8 \quad (38)$$

457 Where  $N$  is the number of data-points we are considering and now  $s$  is the only free variable which  
458 we call the step-size scaling. For approximate methods, we can choose to bypass the MH accept-reject  
459 entirely to speed up computation. If this is done, the algorithm is instead called stochastic gradient  
460 Langevin diffusion (SGLD) [17]. This speeds up computation at the expense of exactness of the  
461 method.

462 Nevertheless, to choose the value of  $s$  we must quantify the trade-off between acceptance ratio and  
463 burn-in time. We do this by way of an example with the primary school dataset [16]. We run the  
464  $b$ -chain for  $T_b = 1,000$  iterations and subsample such that  $\mathcal{T}_b$  is computed with  $\kappa_b = 0.2$  and  $\lambda_b = 5$ .  
465 We then use this to run the  $\theta$ -chain for  $T_\theta = 10,000$  iterations. The acceptance ratio – which we  
466 denote  $r_\alpha$  – is easy enough to compute as simply the fraction of proposed moves which we accept.  
467 However, to quantify burn-in time we must use a different metric. We can plot the mean of the  
468 objective function averaged over all samples as a proxy for burn-in time:

$$\bar{U} := \frac{1}{T_\theta} \sum_{t \in [T_\theta]} U(\theta^{(t)}) \quad (39)$$

469 As the chain will equilibrate in the vicinity of a minima in  $U(\theta)$ , the average over all samples is a  
470 rough indicator of the speed of burn-in. This assumes that the random starting point has high  $U(\theta)$ .  
471 The higher the value of  $\bar{U}$ , the longer the chain took to burn in and reach equilibrium. We plot the  
472 acceptance ratio  $r_\alpha$  and average objective  $\bar{U}$  for 10 values of the step-size multiplier  $s$  logarithmically  
473 spaced in the range  $(10^{-2}, 10^1)$  on figure 5.

474 We see immediately that acceptance ratio  $r_\alpha$  steadily decreases with  $s$ . This is expected as it is  
475 unlikely we stay in a high density region of our target distribution if we are making very large  
476 steps each time. A low acceptance ratio leads to wasted samples and this inefficiency is obviously  
477 undesirable. Nevertheless,  $\bar{U}$  decreases with  $s$  indicating shorter burn-in times for larger step-sizes.  
478 Nevertheless, this effect plateaus for  $s > 0.2$  for this particular dataset. Therefore, we choose  $s = 0.2$   
479 as our step-size multiplier for the primary school datasets as this yields the best trade-off between  $r_\alpha$   
480 and  $\bar{U}$ . Indeed, the acceptance ratio is still high for  $r_\alpha \approx 0.8$  for  $s = 0.2$ . The step-sizes for the other  
481 datasets were chosen following the same argument.

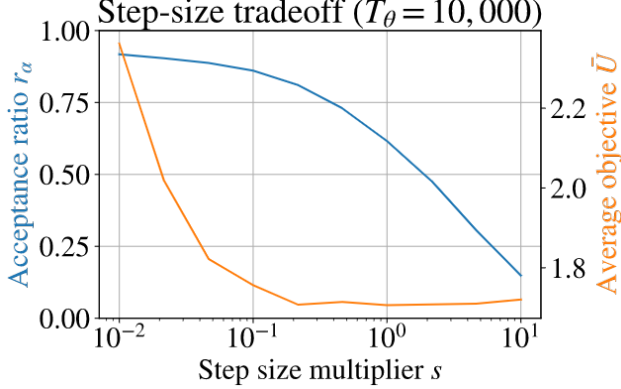


Figure 5: Primary school dataset [16] illustration of step-size tradeoff

### 482 A.3 Burn-in and thinning

483 As with any MCMC method, we must deal with the issues presented by burn-in and thinning. We  
 484 have introduced the notation  $\mathcal{T}_b$  and  $\mathcal{T}_\theta$  to denote the set of samples we keep from the  $b$  and  $\theta$  chains  
 485 respectively. Note that we generate  $\mathcal{T}_b$  and  $\mathcal{T}_\theta$  samples total. The burn-in period refers to the time  
 486 taken for the Markov Chain to converge to the stationary distribution. Sample thinning is necessary  
 487 to ensure that neighbouring samples satisfy independence. However, as we do not leverage the  
 488 independence property this is less important in our analysis. We can write the general set  $\mathcal{T}_*$  as:

$$\mathcal{T}_* = \{T_* \kappa_* + i \lambda_* : 0 \leq i \leq \lfloor T_*(1 - \kappa_*)/\lambda_* \rfloor\} \quad (40)$$

489 Where the parameter  $\kappa_* \in (0, 1)$  controls our burn-in and  $\lambda_*$  controls our thinning.  $\kappa_*$  can be  
 490 determined by plotting the log-target (either  $S(b^{(t)})$  or  $U(\theta^{(t)})$ ) with respect to the epoch  $t$ .  $\kappa_*$  is then  
 491 chosen to encompass the region where the log-target has roughly equilibrated. As we do not leverage  
 492 sample independence  $\lambda_*$  can be chosen less rigorously. We often just use  $\lambda_b = 5$  and  $\lambda_\theta = 10$ .

493 By way of illustration, we can consider the primary school dataset [16]. We plot the normalised  
 494 objective function  $U(\theta^{(t)})/N$  with respect to MALA iteration on figure 6a. We see that the chain  
 495 converges to the modal neighbourhood quickly (within about 2000 iterations of a total 10,000).  
 496 Nevertheless, we pick  $\kappa_\theta = 0.4 > 0.2$  just to be on the safe-side.  $\lambda_\theta = 10$  is chosen somewhat  
 497 arbitrarily as we do not require neighbouring samples to be independent. Nevertheless, this thinning  
 498 does speed up computation of quantities that require an average over all the retained samples – as  
 $|\mathcal{T}_\theta| < T_\theta$ .

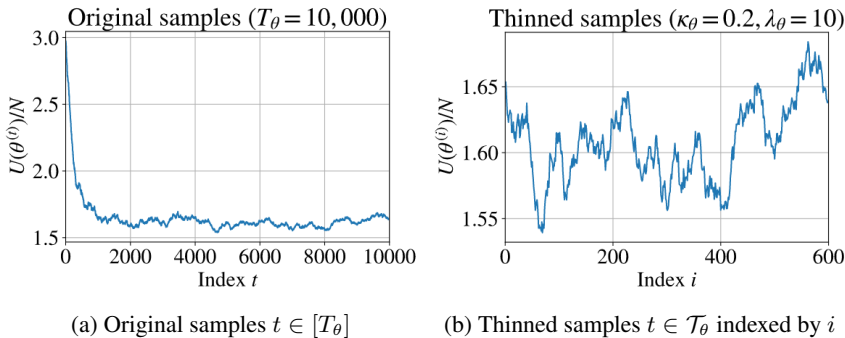


Figure 6: Primary school dataset normalised objective function against sample index

499

500 We see on figure 6b that  $U(\theta^{(i)})$  does bounce around a small amount. This is to be expected we are  
 501 sampling from the posterior rather than converging to the MAP. The variations do appear to be rather  
 502 long in time-scale but we can live with this as we do not require sample independence.

503 **A.4 Initializing the b-chain**

504 For the purposes of our model (the FFBM), the number of blocks  $B$  is a constant which must be  
 505 specified by the data scientist. We could however, allow our choice of  $B$  to be influenced by the  
 506 observed data. This places us in the domain of empirical Bayes, which must be negotiated carefully.  
 507 Prior beliefs must be determined a priori else they are not prior. However, as the number of blocks  
 508 only specifies the coarseness of the analysis, it is fine to allow it to vary. Indeed, Peixoto [10] shows  
 509 that for a fixed average degree the maximum number of detectable blocks scales as  $O(\sqrt{N})$  where  $N$   
 510 is the number of vertices.

511 If we allow  $B$  to vary in the  $b$ -chain (i.e. new blocks can be created and we permit empty blocks) then  
 512 it can be run until a minimum description length (MDL) solution is reached. We take the number of  
 513 non-empty blocks at the MDL to be our fixed block number  $B$  for subsequent analysis. Indeed, it is  
 514 prudent to start our  $b$ -chain at this MDL solution as then we can burn-in time is greatly reduced.

515 **A.5 Dimensionality discussion**

516 There is a challenge when dealing with vertex-features. Many vertex feature often take only one  
 517 of several discrete values within a set. For example, with the primary school dataset [16], a pupil's  
 518 school-class can take one of 10 values from {"1A", "1B", "2A", "2B" ... "5A", "5B"}.

519 It is not immediately obvious how to encode this for the feature-to-block classifier. Although this is  
 520 technically only a single dimension, we choose to expand the data into a set of 10 binary feature flags  
 521  $\in \mathcal{X} = \{0, 1\}$ . Although only one flag will be set at a time it is the simplest method for representing  
 522 discrete-valued data. The reason we choose  $\mathcal{X} = \{0, 1\}$  and not  $\mathcal{X} = \{-1, 1\}$  is that the former  
 523 allows for simpler analysis of the resulting weight values. When a feature is switched off, it has  
 524 no impact on the softmax classifier. It is simpler to only model positive relationships. We prefer to  
 525 say that this block is comprised of the vertices with feature  $d$  on rather than this block contains the  
 526 vertices with feature  $d$  switched off. To make this explicit, say we have a feature encoding a pupil's  
 527 gender: {"male", "female"}, we represent this as 2 binary feature flags "male": {0, 1} and "female":  
 528 {0, 1}. This approach may seem inefficient but it is vital to ensure we can interpret the resulting  
 529 parameter distributions.

530 Nevertheless, this dimensionality expansion means that we cannot include a bias term in our classifier  
 531 as then the MAP solution is less peaked and our  $\theta$ -samples will have higher variance. To illustrate  
 532 this point we need only look at the form of the soft-max classifier with bias vector  $\beta$ , operating on a  
 533 vector  $x$  which only has feature  $d$  turned on such that  $x_i = \mathbb{1}\{i = d\}$ . Component  $j$  of the output is  
 534 given by:

$$\phi_j(x) = \frac{\exp(w_j^T x + \beta_j)}{\sum_{k=1}^B \exp(w_k^T x + \beta_k)} = \frac{\exp(w_{jd} + \beta_j)}{\sum_{k=1}^B \exp(w_{kd} + \beta_k)} \quad (41)$$

535 For the case that  $x$  can only has one entry  $x_d = 1$  and the rest are 0, the term  $w_{kd} + \beta_k$  is effectively  
 536 the new weight for component  $k$ . The bias term  $\beta_k$  becomes an unnecessary extra degree of freedom.  
 537 To illustrate this point, we set  $\beta_k = \beta_0 \forall j$ . If this is the case then equation 41 can be simplified to:

$$\phi_j(x) = \frac{\exp(\beta_0) \cdot \exp(w_{jd})}{\sum_{k=1}^B \exp(\beta_0) \cdot \exp(w_{kd})} = \frac{\exp(w_{jd})}{\sum_{k=1}^B \exp(w_{kd})} \quad (42)$$

538 This expression is independent of  $\beta_0$  and so it is free to vary. This is not the whole picture as we also  
 539 have the prior which introduces a regularisation term which favours weights closer to 0. Nevertheless,  
 540 for mutually exclusive binary feature flags, the bias term does not add to the expressiveness of the  
 541 model and only serves to complicate analysis. We therefore remove the bias term from the Softmax  
 542 classifier. Even for data comprised of several such features (e.g. school class and data) we prefer  
 543 to discard the bias term. The bias term only serves to decrease the loss function by leveraging  
 544 information about the size of each detected block and not feature information. We do not wish to be  
 545 overly confident in our model predictions when such prediction is influenced by block size and not  
 546 feature information. Indeed, the approach was initially developed with a bias term but we found its  
 547 removal yielded more reliable and reproducible results.

548 **B Appendix: Derivations**

549 **B.1 Derivation of conditional block distribution given feature matrix**

550 We wish to determine the form of  $p(b|X)$ . This can be done by integrating over the joint probability  
 551 with respect to  $\theta$ .

$$\begin{aligned} p(b|X) &= \int p(b, \theta|X, \theta)d\theta = \int p(b|X, \theta)p(\theta|X)d\theta \\ &= \int p(b|X, \theta)p(\theta)d\theta = \int \prod_{i \in [N]} \phi_{b_i}(x_i; \theta)p(\theta)d\theta \\ &= \prod_{i \in [N]} \int \frac{\exp(w_{b_i}^T \tilde{x}_i) \prod_{j \in [B]} \mathcal{N}(w_j; 0, \sigma_\theta^2 I)}{\sum_{k \in [B]} \exp(w_k^T \tilde{x}_i)} dw_{1:B} \end{aligned}$$

552 We note that  $b_i \in [B]$  and so the integral's value is unchanged with respect to  $b_i$ . The integrand  
 553 has the same form no matter which value  $b_i$  takes as the prior is the same for each  $w_j$ . As such the  
 554 integral can only be a function of at most  $\tilde{x}_i$  and  $\sigma_\theta^2$  as it is symmetric with respect to  $b_i$  and all the  
 555 various  $w_j$  are integrated out as they are dummy variables. Therefore, denoting the integral by the  
 556 (unknown) function  $f(\tilde{x}_i, \sigma_\theta^2)$ , we write  $p(b|X)$  as follows:

$$p(b|X) = \prod_{i=1}^N f(\tilde{x}_i, \sigma_\theta^2) = \text{const w.r.t } b = c$$

557 As this is a constant with respect to  $b$  we conclude that  $p(b|X)$  must be a uniform distribution.  $1/c$   
 558 is simply the size of the set of values that  $b$  can take. We know  $b_i \in [B]$ . Therefore,  $b \in [B]^N$  and  
 559  $|[B]^N| = B^N = 1/c$ . Putting this all together we conclude that:

$$p(b|X) = B^{-N} \quad (43)$$

560 **B.2 Derivation of U form**

561 The invariant distribution we wish to target for the  $\theta$  samples is the posterior of  $\theta$  given the values of  
 562 the pair  $(X, b)$ . We write this as follows:

$$\pi_\theta(\theta) \propto p(\theta|X, b) \propto p(b|X, \theta)p(\theta) \propto \exp(-U(\theta)) \quad (44)$$

$$\therefore U(\theta) = -(\log p(b|X, \theta) + \log p(\theta)) + \text{const} \quad (45)$$

563 Where we have introduced  $U(\theta)$  equal to the negative log posterior. Each of the constituent terms of  
 564  $U(\theta)$  are easily computed (equation 46) by defining  $y_{ij} := \mathbb{1}\{b_i = j\}$  and  $a_{ij} := \phi_j(x_i; \theta)$ .

$$\log p(b|X, \theta) = \sum_{i \in [N]} \sum_{j \in [B]} y_{ij} \log a_{ij} \quad \text{and} \quad \log p(\theta) = -\frac{(D+1)(B)}{2} \log 2\pi - \frac{1}{2\sigma_\theta^2} \|\theta\|^2 \quad (46)$$

565 Discarding constant terms, we write  $U(\theta)$  as in equation 47. Note that  $\|\theta\|^2 = \sum_i \theta_i^2 = \sum_{j=1}^B \|w_j\|^2$   
 566 is the Euclidean norm of the vector of parameters  $\theta$ .

$$U(\theta) = \left( \sum_{i=1}^N \sum_{j=1}^B y_{ij} \log \frac{1}{a_{ij}} \right) + \frac{1}{2\sigma_\theta^2} \|\theta\|^2 = N \cdot \mathcal{L}(\theta) + \frac{1}{2\sigma_\theta^2} \|\theta\|^2 \quad (47)$$

567 **B.3 Derivation of U gradient with respect to feature parameters**

568 The goal is to determine  $\nabla U(\theta)$ , the gradient of the negative log posterior with respect to the  
 569 parameters. We repeat the form of  $U(\theta)$  in equation 48.

$$U(\theta) = \left( \sum_{i \in [N]} \sum_{j \in [B]} y_{ij} \log \frac{1}{a_{ij}} \right) + \frac{1}{2\sigma_\theta^2} \|\theta\|^2 \quad (48)$$

570 Where  $y_{ij}$  is independent of  $\theta$  and  $a_{ij}$  is the output from the softmax layer, with form as given in  
 571 equation 49.

$$a_{ij} := \phi_j(x_i; \theta) = \frac{\exp(w_j^T \tilde{x}_i)}{\sum_{r \in [B]} \exp(w_r^T \tilde{x}_i)} \quad (49)$$

572 We note that  $\theta = \{w_k\}_{k=1}^B$ , and as such we can write this in vector form  $\theta = [w_1^T, w_2^T \dots w_B^T]^T$ .  
 573 Therefore,  $\nabla U(\theta) = [\partial U / \partial w_1^T, \partial U / \partial w_2^T \dots \partial U / \partial w_B^T]^T$ ; to compute  $\nabla U(\theta)$  it suffices to find the  
 574 form of  $\partial U / \partial w_k$  with respect to a general  $k$ .

575 To this end, we must first find partial derivatives of  $a_{ij}$  and  $\|\theta\|$  with respect to  $w_k$ . Starting with  $a_{ij}$ :

$$\begin{aligned} \frac{\partial a_{ij}}{\partial w_k} &= \frac{\tilde{x}_i \exp(w_j^T \tilde{x}_i) \delta_{jk} \cdot \sum_{r \in [B]} \exp(w_r^T \tilde{x}_i) - \exp(w_j^T \tilde{x}_i) \cdot \tilde{x}_i \exp(w_k^T \tilde{x}_i)}{\left( \sum_{r \in [B]} \exp(w_r^T \tilde{x}_i) \right)^2} \\ &= \tilde{x}_i (a_{ij} \delta_{jk} - a_{ij} a_{ik}) \end{aligned} \quad (50)$$

576 Where  $\delta_{jk} := \mathbb{1}\{j = k\}$ . Now moving onto the derivative of  $\|\theta\|^2$ :

$$\frac{\partial}{\partial w_k} \|\theta\|^2 = \frac{\partial}{\partial w_k} \left( \sum_{r \in [B]} \|w_r\|^2 \right) = 2w_k \quad (51)$$

577 We are ready to put this all together, to find the partial derivative of  $U(\theta)$  with respect to each  $w_k$ :

$$\begin{aligned} \frac{\partial U}{\partial w_k} &= \sum_{i=1}^N \sum_{j=1}^B y_{ij} \left( \frac{-\tilde{x}_i}{a_{ij}} (a_{ij} \delta_{jk} - a_{ij} a_{ik}) \right) + \frac{w_k}{\sigma_\theta^2} \\ &= - \left( \sum_{i=1}^N \tilde{x}_i \left( y_{ik} - a_{ik} \sum_{j=1}^B y_{ij} \right) - \frac{w_k}{\sigma_\theta^2} \right) \\ &= - \left( \sum_{i=1}^N \left\{ \tilde{x}_i (y_{ik} - a_{ik}) \right\} - \frac{w_k}{\sigma_\theta^2} \right) \end{aligned} \quad (52)$$

578 This is the required result. This form can be computed efficiently through matrix operations. The only  
 579 property of  $y_{ij}$  we have used in the derivation is the sum-to-one constraint  $\sum_{j=1}^B y_{ij} = 1$  for all  $i$ .

#### 580 B.4 Hypothesis test on feature weights

581 We are given samples  $\{\theta^{(t)}\}_{t \in \mathcal{T}_\theta} \sim p(\theta | A, X)$  and wish to determine the statistical significance of  
 582 the weights. We adopt matrix notation for simplicity by representing  $\theta$  with the matrix  $B \times D$  matrix  
 583 of feature weights  $W$ . The question is to determine the significance of a particular feature  $d$  by  
 584 examining the value of  $W_{id}$  for all the values  $i \in [B]$ . We know that the posterior is proportional to  
 585 the prior multiplied by the likelihood (assuming that the feature matrix  $X$  is already given):

$$p(\theta | A, X) \propto p(\theta) \cdot p(A | \theta, X) \quad (53)$$

586 The prior term can be evaluated but the likelihood is intractable. The closest we can get is through a  
 587 Monte-Carlo integration over  $b$ :

$$\begin{aligned} p(A | \theta, X) &= \sum_{b \in [B]^N} p(A, b | \theta, X) \\ &= \sum_{b \in [B]^N} p(A | b, \theta, X) \cdot p(b | \theta, X) \\ &= \sum_{b \in [B]^N} p(A | b) \cdot p(b | \theta, X) \\ &\approx \sum_i p(A | b^{(i)}) \quad \text{with } b^{(i)} \sim p(b | \theta, X) \end{aligned} \quad (54)$$

588 This could be implemented for a single value of  $\theta$  but such a form cannot be used to characterise the  
 589 overall form of the posterior. Nevertheless, the form in equation 54 still does highlight something  
 590 interesting. The likelihood is peaked around areas of  $\theta$  that generate a partition  $b$  that is highly likely  
 591 in the SBM sense – high  $p(A|b)$ . This provides the motivation for using the Laplace approximation  
 592 for modelling the posterior  $p(\theta|A, X) \approx p(\theta; \mu, \Sigma)$ . Indeed, the Laplace approximation is often used  
 593 for modelling the posterior in logistic classification [14]. As a simplification we assume that  $\Sigma$  is  
 594 diagonal, therefore each element of  $\theta$  is independent. This assumption does not hold in general but it  
 595 motivates the derivation of the dimensionality reduction we construct by analogy with hypothesis  
 596 testing. Assuming,  $\Sigma$  is diagonal then the posterior for each element of the weight matrix  $W$  can be  
 597 approximated by:

$$p(W_{ij}|A, X) \approx \mathcal{N}(W_{ij}|\hat{\mu}_{ij}, \hat{\sigma}_{ij}^2) \quad (55)$$

598 Where we have used the set of samples for  $W$  drawn according to the exact posterior, to calculate  
 599 unbiased estimates for the mean and standard deviation:

$$\hat{\mu}_{ij} := \frac{1}{|\mathcal{T}_\theta|} \sum_{t \in \mathcal{T}_\theta} W_{ij}^{(t)} \quad \text{and} \quad \hat{\sigma}_{ij}^2 := \frac{1}{|\mathcal{T}_\theta|} \sum_{t \in \mathcal{T}_\theta} (W_{ij}^{(t)} - \hat{\mu}_{ij})^2 \quad (56)$$

600 This approximation is not exact but can show it is accurate empirically. Indeed, if we run the primary  
 601 school experiment with hyper-parameters given in appendix C.2, we can then plot histograms of  
 602 the collected  $W$ -samples and compare these to the Laplace approximation. The results are given on  
 603 figure 7. Even though the Laplace approximation is not exact, it is remarkably reliable.

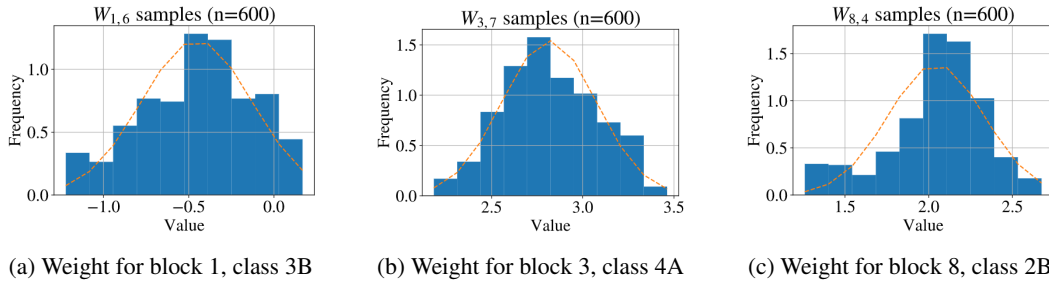


Figure 7: Histograms of sampled weights for the primary school experiment [16]. Dotted line is the applied Laplace approximation.

604 Using the approximation we can construct a test to determine whether a particular weight value has  
 605  $|W_{ij}| > c$  with high probability.

606 **C Appendix: Implementation details**

607 **C.1 Algorithms**

---

**Algorithm 1** Block membership sample generation

---

```

procedure SAMPLEBLOCKMEMBERSHIPS( $A, T_b$ )
     $b^{(0)} \leftarrow \arg \min_b S(b|A)$                                  $\triangleright$  Implemented as greedy heuristic in graph-tool library
    for  $t \in \{0, 1 \dots T_b - 1\}$  do
         $b' \leftarrow \sim q_b(b^{(t)}, b'|A)$ 
         $\log \alpha_b \leftarrow \log \alpha_b(b^{(t)}, b'|A)$ 
         $\eta \leftarrow \sim \text{Unif}(0, 1)$ 
        if  $\log \eta < \log \alpha_b$  then
             $b^{(t+1)} \leftarrow b'$ 
        else
             $b^{(t+1)} \leftarrow b^{(t)}$ 
        end if
    end for
    return  $\{b^{(t)}\}_{t=1}^{T_b}$ 
end procedure

```

---

**Algorithm 2** FFBM parameter pseudo-marginal inference

---

```

procedure SAMPLEFEATUREWEIGHTS( $X, \{b^{(t)}\}, T_b, \sigma_\theta, s$ )
     $\hat{Y}_{ij} \leftarrow \frac{1}{|\mathcal{T}_b|} \sum_{t \in \mathcal{T}_b} \mathbb{1}\{b_i^{(t)} = j\} \quad \forall i, j$ 
     $\theta^{(0)} \leftarrow \sim \mathcal{N}(0, \sigma_\theta I)$ 

    for  $t \in \{0, 1 \dots T_\theta - 1\}$  do
         $\xi \leftarrow \sim \mathcal{N}(0, I)$ 
         $h_t \leftarrow \frac{s}{N} \cdot 250(1000 + t)^{-0.8}$ 
         $g_t \leftarrow \nabla U(\theta^{(t)}|X, \hat{Y})$ 

         $\theta' \leftarrow \theta^{(t)} - h_t \cdot g_t + \sqrt{2h_t} \cdot \xi$ 
         $\log \alpha_\theta \leftarrow \log \alpha_\theta(\theta^{(t)}, \theta'|A, \hat{Y})$ 
         $\eta \leftarrow \sim \text{Unif}(0, 1)$ 
        if  $\log \eta < \log \alpha_\theta$  then
             $\theta^{(t+1)} \leftarrow \theta'$ 
        else
             $\theta^{(t+1)} \leftarrow \theta^{(t)}$ 
        end if
    end for
    return  $\{\theta^{(t)}\}_{t=1}^{T_\theta}$ 
end procedure

```

---

---

**Algorithm 3** Dimensionality reduction

---

```

procedure REDUCEDIMENSION( $\{W^{(t)}\}, \mathcal{T}_\theta, k, D'$ )
     $(B, D) \leftarrow W^{(0)}.shape$ 
     $\hat{\mu}_{ij} \leftarrow \frac{1}{|\mathcal{T}_\theta|} \sum_{t \in \mathcal{T}_\theta} W_{ij}^{(t)} \quad \forall i \in [B], j \in [D]$ 
     $\hat{\sigma}_{ij} \leftarrow \frac{1}{|\mathcal{T}_\theta|} \sum_{t \in \mathcal{T}_\theta} \left( W_{ij}^{(t)} - \hat{\mu}_{ij} \right)^2 \quad \forall i \in [B], j \in [D]$ 

    for  $d \in [D]$  do
        for  $i \in [B]$  do
             $l_i \leftarrow \hat{\mu}_{id} - k \cdot \hat{\sigma}_{id}$ 
             $u_i \leftarrow \hat{\mu}_{id} + k \cdot \hat{\sigma}_{id}$ 
            if  $l_i \leq 0$  and  $u_i \geq 0$  then
                 $l_i, u_i \leftarrow 0$ 
            end if
        end for
         $c_d \leftarrow \max_i \min(|l_i|, |u_i|)$ 
    end for

    indexArray  $\leftarrow$  indexSort( $c$ , descending=True)[ $0 : D'$ ]
     $d^* \leftarrow$  indexArray[-1]
     $\mathcal{D}' \leftarrow$  Set(indexArray)
     $c^* \leftarrow c_{d^*}$ 
    return  $\mathcal{D}', c^*$ 
end procedure

```

---

608    **C.2 Hyperparameter values**

Table 2: Hyper-parameter values for each experiment

| Dataset   | $B$ | $f$ | $\sigma_\theta$ | $T_b$ | $\kappa_b$ | $\lambda_b$ | $T_\theta$ | $\kappa_\theta$ | $\lambda_\theta$ | $s$   | $k$ | $D'$ | $T'_\theta$ | $\kappa'_\theta$ | $\lambda'_\theta$ | $s'$ |
|-----------|-----|-----|-----------------|-------|------------|-------------|------------|-----------------|------------------|-------|-----|------|-------------|------------------|-------------------|------|
| Polbooks  | 3   | 0.7 | 1               | 1,000 | 0.2        | 5           | 10,000     | 0.4             | 10               | 0.05  | —   | —    | —           | —                | —                 | —    |
| School    | 10  | 0.7 | 1               | 1,000 | 0.2        | 5           | 10,000     | 0.4             | 10               | 0.2   | 1   | 10   | 10,000      | 0.4              | 10                | 0.2  |
| FB Egonet | 10  | 0.7 | 1               | 1,000 | 0.2        | 5           | 10,000     | 0.4             | 10               | 0.017 | 1   | 10   | 10,000      | 0.4              | 10                | 0.5  |

609    **C.3 Hardware specification**

610 All data analysis and visualisation was implemented in Python. Full source code is available in the  
611 supplementary material. The scripts were run using a standard PC using the Windows Subsystem for  
612 Linux (WSL) environment. Specs are:

- 613     • **CPU:** Intel(R) Core(TM) i7-1065G7
- 614     • **RAM:** 8GB
- 615     • **GPU:** Intel(R) Iris(R) Plus Graphics

616 On this hardware each experiment iteration took the following amount of time to execute:

Table 3: Compute-time for each experiment

| Dataset   | $b$ -chain | $\theta$ -chain | Reduced $\theta$ -chain | Overall compute time |
|-----------|------------|-----------------|-------------------------|----------------------|
| Polbooks  | ~1s        | ~10s            | —                       | ~11s                 |
| School    | ~1s        | ~7s             | ~7s                     | ~15s                 |
| FB Egonet | ~2s        | ~50s            | ~8s                     | ~60s                 |